Synthesis and Characterization of Zn(II), Cu(II), and Ni(II)-Levofloxacin Complexes for Carbon Dioxide Storage Media

Hadeel Adil[1], Hamsa Thamer[1], Dina Saadi Ahmed[2], Raghda Alsayed[1], Muna Bufaroosha[3*], Khalid Zainulabdeen[1], Hassan Hashim[4], Alaa Mohammed[5], and Emad Yousif[1]**

[1]*Department of Chemistry, College of Science, Al-Nahrain University, Baghdad 64021, Iraq*

[2]*Department of Chemical Industries, Institute of Technology-Baghdad, Middle Technical University, Baghdad 10074, Iraq*

[3]*Department of Chemistry, College of Science, United Arab Emirates University, Al-Ain 1818, United Arab Emirates*

[4]*Department of Physics, College of Science, Al-Nahrain University, Baghdad 64040, Iraq*

[5]*Department of Environmental Science, College of Energy and Environmental Science, Alkarkh University of Science, Baghdad 10081, Iraq*

* ***Corresponding author:***

email: muna.bufaroosha@uaeu.ac.ae; emad_yousif@hotmail.com***

Received: May 17, 2023
Accepted: July 5, 2023

DOI: 10.22146/ijc.84552

Abstract: *Three complexes ([$CuL_2(H_2O)_2$], [$NiL_2(H_2O)_2$], and [ZnL_2Cl_2]) have been synthesized through the reaction of metal salts and levofloxacin and characterized by spectrophotometers. The morphology of the complexes was investigated using field emission scanning electron microscopy (FESEM). The physicochemical properties of these complexes were evaluated using the Brunauer-Emmett-Teller (BET) and Barrett-Joyner-Halenda (BJH) techniques. Furthermore, the storage capacity of these complexes was verified using the H-sorb 2600 analyzer at a temperature of 323 K and varying pressure conditions. The obtained data substantiates that the synthesized complexes exhibit favorable attributes for CO_2 absorption. The surface area reaches 24.97 m^2/g with capacities of 123.073 m^3/g and 34.400 m^3/g to adsorb CO_2. The escalating levels of CO_2 in the atmosphere, primarily resulting from the combustion of fossil fuels to meet the surging energy requirements, pose a pressing environmental challenge. Consequently, there has been a surge in research focused on the development of novel materials aimed at facilitating CO_2 storage.*

Keywords: *levofloxacin; gas storage; global warming; carbon dioxide uptake*

INTRODUCTION

According to several chemical methods, abundant porous materials have been synthesized [1]. Such of these materials are zeolites, carbons, porous polymers and metal-organic frameworks (MOFs). Many properties, such as pore size and surface area of porous materials, might be affected according to functional groups (e.g., hydroxyl groups), heteroatoms, aromatic rings, polar groups, and polymeric chains which these materials contain, and could increase the interactions with gas molecules [2-3]. Recently, many studies applied porous materials in different fields, including catalysis, environmental protection, biology, energy saving and conserving [1]. Over the past years, many MOF materials have been prepared, characterized, and applied in different fields. MOF materials could be produced from the formation of coordination bonds between metal and organic molecules [3]. The affinity of the metals to bind with different organic molecules makes the possibility to prepare thousands of these compounds [4].

Over time, several developments were made in the chemistry of MOF materials, which included geometric shapes such as octahedral and tetrahedral. This, in turn, can be affected by the expansion of coordination bonds between a metal and organic molecules [5]. The organic molecules might be carboxylates, phosphate, sulfonate and *N*-containing heterocyclic [6]. In 1990, the first investigation of the porosity of MOF materials was achieved at high pressure to force the gas molecules to be absorbed on the material's surfaces [7]. The adsorption and desorption measurements of molecules of gas at high and low pressure and temperature prove the permanent porosity of the materials. The first proof was carried out on zinc terephthalate MOF by measuring the nitrogen and carbon dioxide (CO_2) isotherms [8-9].

One of the most common applications of MOF materials is gas storage media [6,10-12]. In the last decades, thousands of studies were performed on the ability of MOFs to absorb and store H_2, CO_2, and CH_4 [13-15]. In particular, CO_2 capture has become the focus of many studies because the industrial revolution and consumption of fossil fuels lead to the increase in the levels of CO_2, which is the major greenhouse as well as leads to "global warming" [16]. In 2015 the National Oceanic and Atmospheric Administration (NOAA) reported that the concentration of CO_2 in the atmosphere reached 403 ppm, which increase of about 25% than in 1958 [17]. In a recent study, several materials have been synthesized which can absorb, store and regenerate greenhouse gases to reduce their level in the atmosphere [18-21].

Several processes have been used to synthesize novel MOFs with high surface areas by using huge and longer organic molecule structures [22]. The studies revealed that the high gravimetric gas uptake by MOFs is proportional to the high surface area and porosity under high pressure [23-25]. As an illustration, M-MOF-74 (M = Mg, Co, Fe, Zn, or Ni) has been synthesized with a large surface area that is measured using the BET method, making it able to capture CO_2 [26]. The acid-base and dipole-quadrupole interactions between the N sites and CO_2 gas molecules would stimulate CO_2 absorption when using the *N*-containing ligands [12]. On the other hand, the electrostatic interactions with the CO_2 quadrupole moment would be enhanced by the presence of water molecules that coordinated with metal. The metal acts as Lewis acid by having partial positive charges on its sites, resulting in a strong interaction between the coordinately unsaturated metal sites and CO_2 molecules [27]. The structural characteristics of MOF materials that have a large capacity for strong binding sites, which facilitate strong interactions with gas molecules, are distinguished by the hybridization of metal [28].

Zeolite, a CO_2 capture material, has garnered significant attention among researchers. Previous studies have highlighted its notable capacity for adsorbing CO_2 under conditions of 25 °C and low pressure [29-30]. Levofloxacin complexes were considered for gas capture and the inspiration for our research since these compounds' capacities to adsorb gas vary depending on their physical and chemical characteristics. In the pursuit of novel adsorbents for CO_2 capture, our research focus shifted towards heterocyclic compounds, owing to their inherent utility as biologically active substances. Given the potential benefits of these attributes in the realm of CO_2 adsorption, we embarked on synthesizing fresh levofloxacin metal complexes, followed by an extensive investigation into their applicability in the field of CO_2 capture.

■ EXPERIMENTAL SECTION

Materials

The materials used in this study were levofloxacin, metal salts ($ZnCl_2$, $NiCl_2·6H_2O$, $CuCl_2·6H_2O$), and methanol, which were ordered from Sigma-Aldrich (Schnelldorf, Bavaria, Germany).

Instrumentation

The Fourier transform infrared (FTIR) spectra of the metal complexes were carried out on FTIR 8300 Shimadzu spectrophotometer using KBr pellets at 400–4000 cm^{-1} (Tokyo, Japan). Shimadzu UV-1601 spectrophotometer was utilized to examine the metal complexes' UV-visible absorption spectra in methanol (Tokyo, Japan). Furthermore, a typical portable conductivity meter, the WTW ProfiLine Oxi 3205, (Xylem Inc., Weinheim, Germany), was used to measure the conductivity of the metal complexes in ethanol at a temperature of 25 °C. In addition, a Bruker BM6 magnetic balance (Bruker, Zürich, Switzerland) was employed to test the magnetic susceptibilities of the metal complexes. Finally, in order to analyze the surface morphology of the metal complexes, ZEISS was applied in conjunction with dispersive X-ray (EDX) and field emission scanning electron microscopy (FESEM) investigations.

Procedure

Metal complexes preparation

A suitable amount of metal salts of $ZnCl_2$ (1.0 mmol, 0.1363 g), $NiCl_2·6H_2O$ (1.0 mmol, 0.2377 g) or $CuCl_2·6H_2O$ (1.0 mmol, 0.2425 g) was dissolved in 5 mL of methanol and then added to a solution of levofloxacin (5 mL of MeOH, 2.0 mmol (0.7228 g) of levofloxacin) as illustrated in Schemes 1 and 2. The mixture was heated for 3 h under reflux. After cooling, the solid was filtered, washed with MeOH, and then recrystallized from ethanol to produce the required metal complex. The complexes' measured yield percentages, colors, and melting points are displayed in Table 1.

Porosity and surface area of complexes

The MicroActive for TriStar II Plus Version 2.03 model of Micromeritics analyzers was utilized to investigate the nitrogen adsorption-desorption isotherms for the complexes. The Brunauer-Emmett-Teller (BET) method and the Barrett-Joyner-Halenda (BJH) theory were employed to analyze and estimate the specific pore volumes, diameter, and pore size distribution of the metal complexes.

Gas adsorption analysis

An H-sorb 2600 high-pressure volumetric adsorption analyzer was applied to calculate the volumetric amount of CO_2 gas that the complexes adsorbed.

■ RESULTS AND DISCUSSION

Characterizing Metal(II) Complexes

The synthesized complexes are characterized by FTIR and UV-vis spectroscopy. The mean data of FTIR spectra are summarized in Table 2. FTIR spectrum of

Table 1. Physical properties and yield percentages of the complexes

Compounds	Color	M.P. (°C)	Yield%
L	White	213–218 (dec.)	-
$[CuL_2(H_2O)_2]$	Blue	280–282	81
$[NiL_2(H_2O)_2]$	Green	300 (dec.)	79
$[ZnL_2Cl_2]$	White	220 (dec.)	83

Table 2. Ligand and synthetic complex FTIR data values

Compounds	Wavenumber (cm^{-1})		
	$C{=}O_{(sym)}$	$C{=}O_{(asym)}$	$\Delta\nu_{(asym-sym)}$
L	1440	1614	-
$[CuL_2(H_2O)_2]$	1445	1612	167
$[NiL_2(H_2O)_2]$	1454	1611	157
$[ZnL_2]$	1468	1613	145

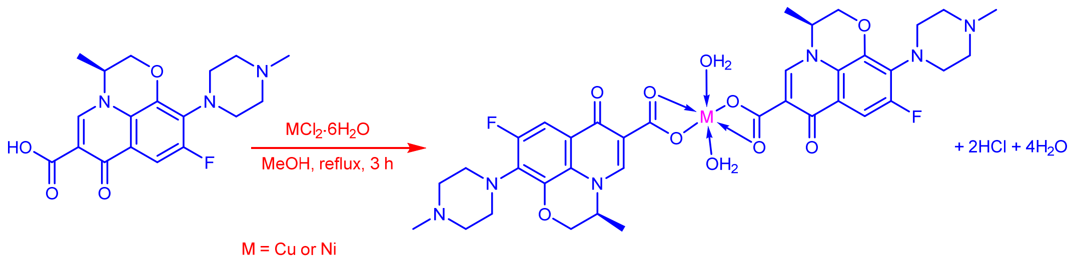

Scheme 1. Synthesis of Cu and Ni complexes

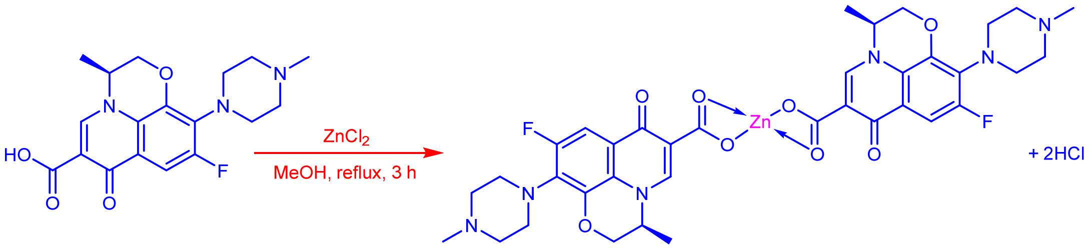

Scheme 2. Synthesis of Zn complexes

ligand, where observed the resonance frequency of symmetry and asymmetry of carbonyl carboxylic acid at 1440 and 1614 cm^{-1}. The synthesized complexes spectra show the difference between asymmetry ($\nu_{(asym)}$) and symmetry ($\nu_{(sym)}$) ranging from 145 to 167 cm^{-1}, which indicates that the ligand was bidentate.

The mean data of UV-vis spectroscopy are tabulated in Table 3. The absorption bands of the ligand spectrum observed at 34,843 and 33,557 cm^{-1} correspond to $\pi\rightarrow\pi^*$ and $n\rightarrow\pi^*$ transitions. The spectrum of the Cu(II) complex shows bands at 29,674 cm^{-1} due to the LMCT (ligand to metal charge transfer), and 27,027 belong to $2Eg\rightarrow 2T_2g$ transition. These bands are attributed to distorted octahedral geometry. The electronic spectrum of the Ni(II) complex reveals a band at 29,940 cm^{-1} for the $3A_2g$ (F)→$3T_1g$ (P) transition, while the $3A_2g$ (F)→$3T_1g$ (F) transition occurs at 26,882 cm^{-1} for high spin octahedral geometry with magnetic susceptibility 2.9 BM. In the end, the electronic spectrum of the Zn(II) complex displays bands at 29,674 and 27,248 cm^{-1} due to the charge transfer. The suggested geometry is tetrahedral with the magnetic susceptibility value zero. Based on the molar conductivity (Λ_m) measurements, the results reveal that the complexes were nonelectrolytes [31], and the values ranged from 5 to 22 μS/cm. The UV-vis spectra, magnetic susceptibility ($\mu_{eff.}$) and conductivity of the complexes indicate the suggested geometries.

Surface Morphology of Metal(II) Complexes

FESEM was used to examine the complicated surfaces. Fig. 1 presents the FESEM images of the synthesized complexes at 1 μm magnification level. It is evident from the images that the surfaces of the complexes exhibit a uniform structure and feature various porous formations characterized by distinct particle sizes.

Table 3. Electronic transitions, absorption band energies, magnetic moments, geometry, conductivity, and hybridization

Complexes	Λ (nm)	Absorption band (cm^{-1})	Transitions	Λ_m (μS/cm)	$\mu_{eff.}$	Geometry	Hybridization
L	287	34,843	$\pi\rightarrow\pi^*$	-	-	-	-
	298	33,557	$n\rightarrow\pi^*$				
$CuL_2{\cdot}2H_2O$	285	35,088	$\pi\rightarrow\pi^*$	22	1.8	Distorted Octahedral	sp^3d^2
	296	33,784	$n\rightarrow\pi^*$				
	337	29,674	LM CT				
	370	27,027	$^2Eg\rightarrow{}^2T_2g$				
$NiL_2{\cdot}2H_2O$	283	35,336	$\pi\rightarrow\pi^*$	5	2.9	Octahedral	sp^3d^2 high spin
	296	33,784	$n\rightarrow\pi^*$				
	334	29,940	^3A_2g (F)→^3T_1g (P)				
	372	26,882	^3A_2g (F)→^3T_1g (F)				
ZnL_2	286	34,965	$\pi\rightarrow\pi^*$	13	0	Tetrahedral	sp^3 diamagnetic
	296	33,784	$n\rightarrow\pi^*$				
	337	29,674	CT				
	367	27,248					

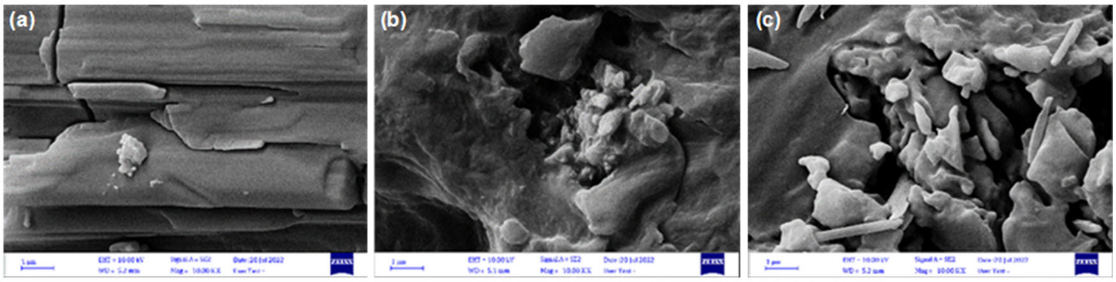

Fig 1. FESEM images of (a) Cu(II), (b) Ni(II), and (c) Zn(II) complexes

EDX analysis was used to determine the elemental composition of complex surfaces. SEM, a common technique in chemical microanalysis, is combined with EDX to determine the chemical structure of produced compounds. The elemental composition of the synthesized complexes was determined based on the EDX mapping, as summarized in Table 4. The EDX data exhibited highly abundant absorption bands corresponding to the carbon atoms, as well as those for N and F from levofloxacin, but in lower proportions.

In order to corroborate the findings of atomic force microscopy (AFM) experiments regarding the porosity of materials exhibiting notable average roughness, characterized by rough surfaces and a prominent porous structure, emphasis was placed on complexes incorporating elevated levels of heteroatoms and aromatic residues. These particular complexes demonstrated enhanced efficacy in reducing surface roughness. Employing this method enables the acquisition of precise information pertaining to the geometric attributes of particles. Zn complex, specifically, exhibits a marked degree of porosity and possesses a high Rq value. The AFM images of the complexes are presented in Fig. 2.

Levofloxacin metal complexes with a high level of heteroatoms and aromaticity resulted in greater improvement in the Rq.

Gas Adsorption Isotherm Measurements

The specific surface area, porosity, and storage capacity were evaluated by N_2 and CO_2 isotherms measurement. The adsorption of N_2 on the solid surface of the produced complexes determines the specific surface

Table 4. EDX data for levofloxacin metal complexes

Complex	%C	%N	%F	%M
$CuL_2{\cdot}2H_2O$	52.8	10.2	4.6	7.7
$NiL_2{\cdot}2H_2O$	53.1	10.3	4.6	7.2
ZnL_2	55.0	10.6	4.8	8.3

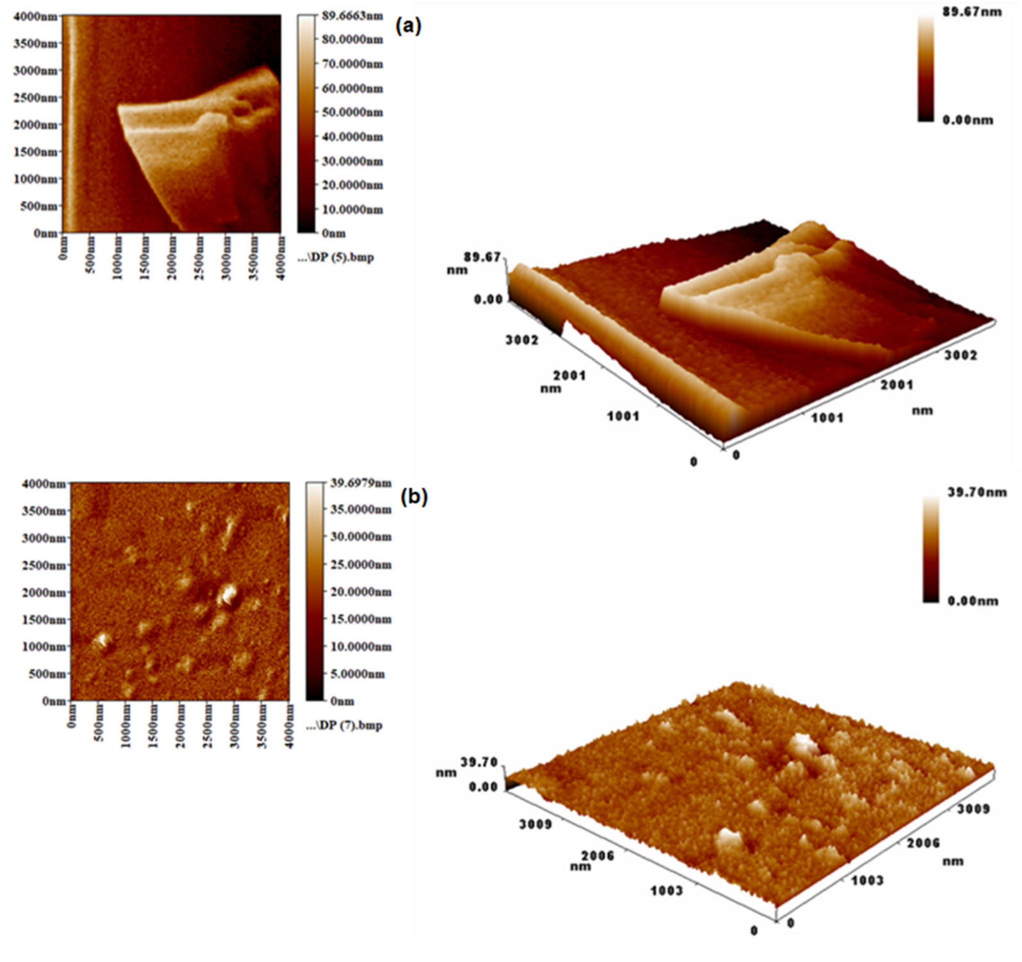

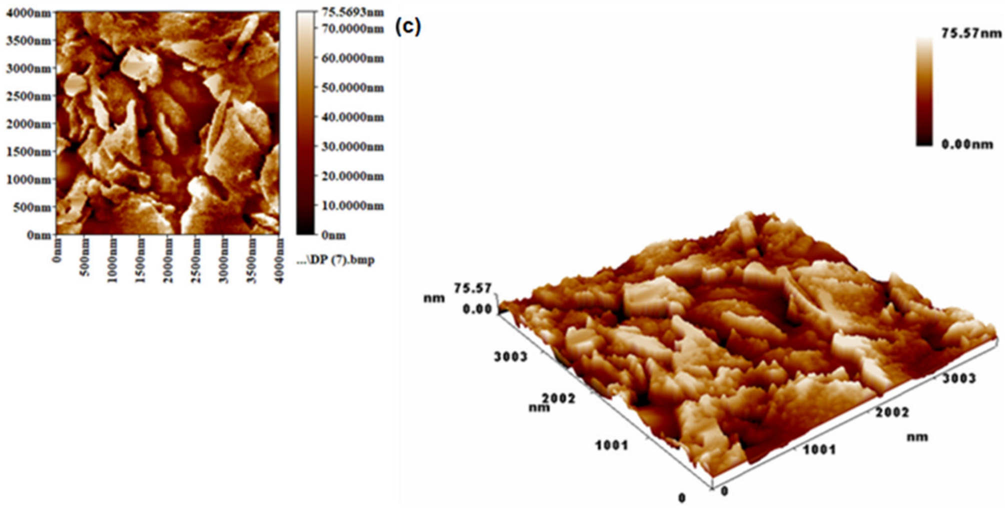

Fig 2. AFM images of (a) Cu(II), (b) Ni(II), and (c) Zn(II) complexes

area and porosity parameters based on BET and BJH techniques [32]. The measurements were carried out at 77 K and 88 kPa. The complexes' N_2 adsorption-desorption isotherms are shown in Fig. 3, where the amount of gas absorbed rises as pressure is increased. According to the IUPAC recommendation, the adsorption-desorption isotherms of the Cu(II) and Zn(II) complexes belong to the type IV isotherm, while the Ni(II) complex has a type V isotherm. Hysteresis attributed to the materials' mesoporosity can be recognized in types IV and V isotherms [33].

Fig. 4 shows the relationship between pore size distribution and pore size width. The pore diameter ranged between 2.1 and 83.9 nm, corresponding to mesopores [34]. As tabulated in Table 5, the specific surface area of the complexes varies from 0.818 to 24.97 m^2/g, while the best amount uptake of N_2 is carried by the Zn(II) complex, which reaches 123.073 m^3/g.

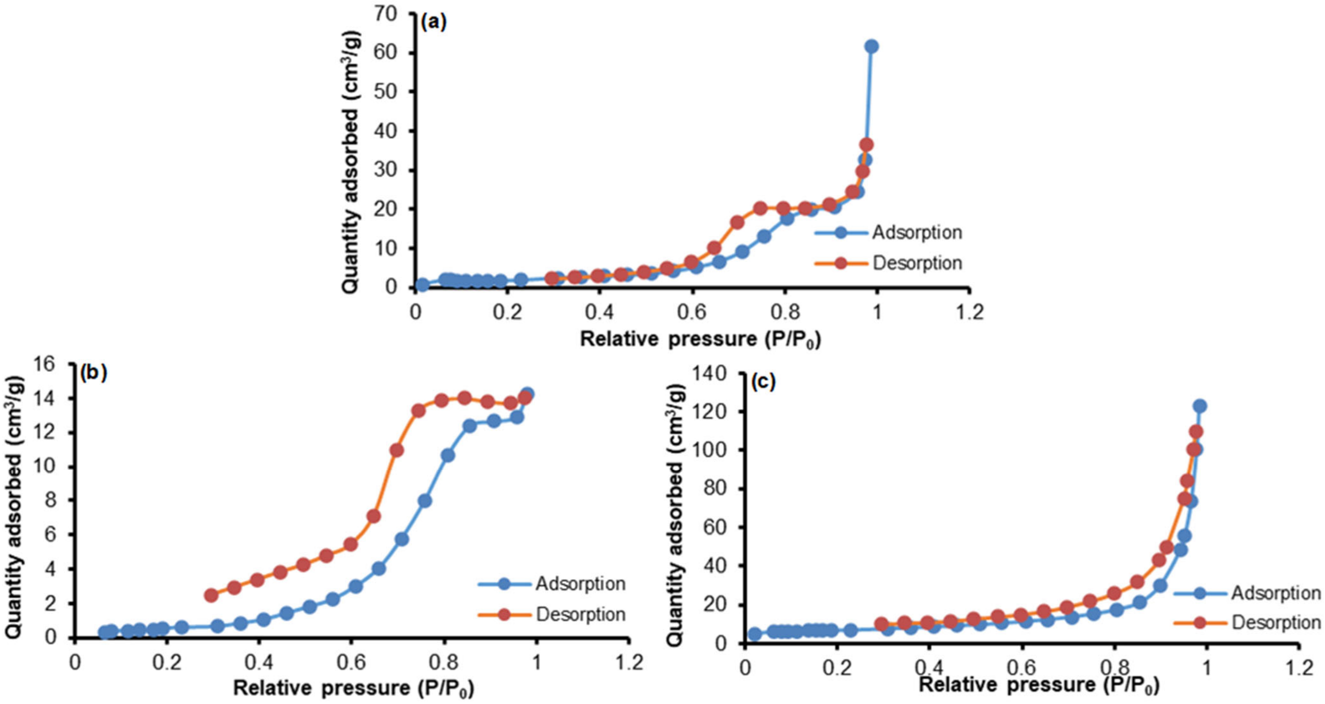

Fig 3. Metal complexes' N_2 adsorption-desorption isotherms on a) Cu(II), b) Ni(II), and c) Zn(II)

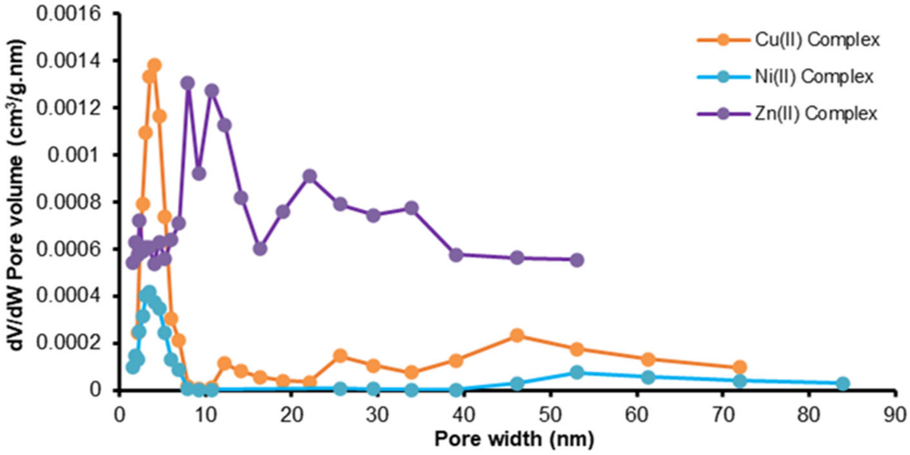

Fig 4. Metal complex's pore size and pore-volume distribution

In another hand, the CO_2 adsorption isotherm for the complexes of the metals has been determined at 323 K and 50 bar, as exhibited in Fig. 5. The Zn(II) complex observed high efficiency in storing CO_2 with a capacity of 34.40 cm^3/g, as illustrated in Table 5. The presence of heteroatoms and aromatic rings enhances the interactions with gas molecules [35]. The metals play a very important role in making the complexes more sufficient to capture the gas molecules. In the case of the unsaturated metal sites, a strong interaction with CO_2 molecules could occur, as exhibited by Zn(II) complex [27]. Ultimately, within the context of acid-base chemistry, the metals function as Lewis acids, while CO_2 acts as a Lewis base [36-37]. This interaction is characterized by the inherent acid-base properties of CO_2.

The complexes that were produced performed remarkably well as CO_2 gas adsorbent surfaces. This is because the surface of synthetic materials and CO_2 molecules form robust van der Waals and dipole-dipole interactions.

The capacity for gas absorption of the synthesized complex was evaluated using a high-pressure volumetric adsorption apparatus of type H-sorb 2600. To eliminate any solvent or water traces that may have been trapped inside the pores, the complexes were degassed under

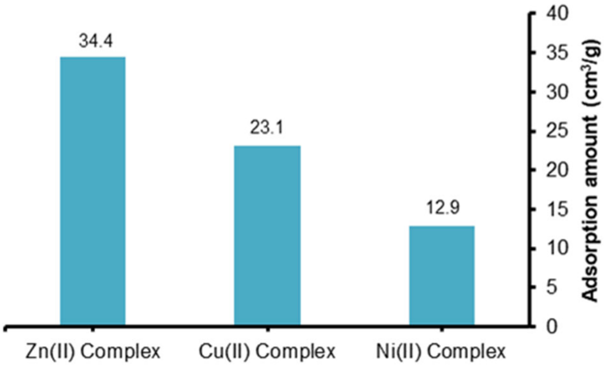

Fig 5. CO_2 adsorption isotherm of metal(II) complexes

Table 5. Porosity properties, specific surface area, and capacity storage of metal complexes and other materials for different studies

Complexes	S_{BET} (m^2/g)	N_2 adsorption (cm^3/g)	Average pore diameter (nm)	Total pore volume (cm^3/g)	CO_2 adsorption (cm^3/g)	Ref.
$CuL_2 \cdot 2H_2O$	12.188	61.77	31.357	0.0116950	23.1	Current project
$NiL_2 \cdot 2H_2O$	0.818	14.00	66.640	0.0033791	12.9	
ZnL_2	24.970	123.07	30.493	0.0418390	34.4	
$NiL_2 \cdot 2H_2O$	22.750	85.45	12.470	0.1080000	34.5	[10]
COF-1	4.682	2.71	34.901	0.0100720	26.3	[38]
Schiff base 1	17.990	5.50	17.020	0.0083000	31.4	[39]
Coumarins	-	-	-	-	31.0	[40]

vacuum and heat using an oven that was run at 50 °C for 1 h. The gas absorption examination was repeated under similar circumstances for the prepared complex to achieve precise data and determine the ideal pressure. The degree of interactions between the adsorbent and adsorbate, such as hydrogen bonds and van der Waals forces, as well as the kind of ligand and the size of the pores, all affect the adsorption of gases. Due to the high quadrupole moment of CO_2, high uptake of CO_2 may also be facilitated by electrostatic forces (van der Waals forces and the polarization force and surface field-molecular dipole interactions). The capacity storage of metal complexes and other materials for different studies is presented in Table 5.

■ CONCLUSION

The relevant complexes were produced via the reaction of levofloxacin with metal salts. Recrystallization was used to purify the products, and FTIR and UV-vis spectroscopy were performed to confirm the chemical composition of the pure chemicals. The peaks required to demonstrate the levofloxacin metal complexes' chemical structure were all adequately validated. Levofloxacin metal complexes with a levofloxacin moiety are produced using a quick and easy procedure. Three complexes were synthesized, characterized and applied as gas storage media. SEM images of the produced materials exhibited a variety of porosity diameters. Additionally, they showed a small collection of particles of various sizes and shapes. The gas adsorption isotherms observed that these complexes are suitable for CO_2 uptake. The Zn(II) complex has a high efficiency to adsorb gas molecules compared to Cu(II) and Ni(II) complexes, due to its high surface area and affinity towards the gas molecules.

■ ACKNOWLEDGMENTS

We thank Al-Nahrain, Middle Technical, United Arab Emirates and AL-Karkh Universities for technical support.

■ AUTHOR CONTRIBUTIONS

Dina S. Ahmed: investigation, original draft preparation, review and editing. Emad Yousif: conceptualization, methodology, software, validation, formal analysis, resources, data curation, funding, original draft preparation, review and editing. Hadeel Adil, Hamsa Thamer and Raghda Alsayed: methodology, software, validation, formal analysis, data curation, original draft preparation, review and editing. Muna Bufaroosha, Khalid Zainulabdeen and Alaa Mohammed: investigation, original draft preparation, review and editing. Hassan Hashim: software, validation, formal analysis, original draft preparation, review and editing.

■ REFERENCES

[1] dos Reis, G.S., Guy, M., Mathieu, M., Jebrane, M., Lima, E.C., Thyrel, M., Dotto, G.L., and Larsson, S.H., 2022, A comparative study of chemical treatment by $MgCl_2$, $ZnSO_4$, $ZnCl_2$, and KOH on physicochemical properties and acetaminophen adsorption performance of biobased porous materials from tree bark residues, *Colloids Surf., A*, 642, 128626.

[2] Wang, W., Zhou, M., and Yuan, D., 2017, Carbon dioxide capture in amorphous porous organic polymers, *J. Mater. Chem. A*, 5 (4), 1334–1347.

[3] Cai, G., Yan, P., Zhang, L., Zhou, H.C., and Jiang, H.L., 2021, Metal–organic framework-based hierarchically porous materials: Synthesis and applications, *Chem. Rev.*, 121 (20), 12278–12326.

[4] Li, H., Wang, K., Sun, Y., Lollar, C.T., Li, J., and Zhou, H.C., 2018, Recent advances in gas storage and separation using metal–organic frameworks, *Mater. Today*, 21 (2), 108–121.

[5] Wen, M., Li, G., Liu, H., Chen, J., An, T., and Yamashita, H., 2019, Metal–organic framework-based nanomaterials for adsorption and photocatalytic degradation of gaseous pollutants: Recent progress and challenges, *Environ. Sci.: Nano*, 6 (4), 1006–1025.

[6] Li, B., Wen, H.M., Zhou, W., and Chen, B., 2014, Porous metal–organic frameworks for gas storage and separation: What, how, and why?, *J. Phys. Chem. Lett.*, 5 (20), 3468–3479.

[7] Mason, J.A., Veenstra, M., and Long, J.R., 2014, Evaluating metal–organic frameworks for natural gas storage, *Chem. Sci.*, 5 (1), 32–51.

[8] Sanz, R., Martínez, F., Orcajo, G., Wojtas, L., and Briones, D., 2013, Synthesis of a honeycomb-like Cu-based metal–organic framework and its carbon dioxide adsorption behaviour, *Dalton Trans.*, 42 (7), 2392–2398.

[9] Mohammed, A., Ahmed, A.U., Ibraheem, H., Kadhom, M., and Yousif, E., 2022, Physisorption theory of surface area and porosity determination: A short review, *AIP Conf. Proc.*, 2450 (1), 020007.

[10] Baumann, A.E., Burns, D.A., Liu, B., and Thoi, V.S., 2019, Metal-organic framework functionalization and design strategies for advanced electrochemical energy storage devices, *Commun. Chem.*, 2 (1), 86.

[11] Ma, S., and Zhou, H.C., 2010, Gas storage in porous metal–organic frameworks for clean energy applications, *Chem. Commun.*, 46 (1), 44–53.

[12] Lin, Y., Kong, C., Zhang, Q., and Chen, L., 2017, Metal-organic frameworks for carbon dioxide capture and methane storage, *Adv. Energy Mater.*, 7 (4), 1601296.

[13] Demir, H., Aksu, G.O., Gulbalkan, H.C., and Keskin, S., 2022, MOF membranes for CO_2 capture: Past, present and future, *Carbon Capture Sci. Technol.*, 2, 100026.

[14] Rosli, A., and Low, S.C., 2020, Molecularly engineered switchable photo-responsive membrane in gas separation for environmental protection, *Environ. Eng. Res.*, 25 (4), 447–461.

[15] Chaemchuen, S., Kabir, N.A., Zhou, K., and Verpoort, F., 2013, Metal–organic frameworks for upgrading biogas via CO_2 adsorption to biogas green energy, *Chem. Soc. Rev.*, 42 (24), 9304–9332.

[16] Latake, P.T., Pawar, P., and Ranveer, A.C., 2015, The greenhouse effect and its impacts on environment, *Int. J. Innovative Res. Creat. Technol.*, 1 (3), 333–337.

[17] Ma, L., Chen, S., Qin, C., Chen, S., Yuan, W., Zhou, X., and Ran, J., 2021, Understanding the effect of H_2S on the capture of CO_2 using K-doped Li_4SiO_4 sorbent, *Fuel*, 283, 119364.

[18] Yan, Y., Yang, S., Blake, A.J., and Schröder, M., 2014, Studies on metal–organic frameworks of Cu(II) with isophthalate linkers for hydrogen storage, *Acc. Chem. Res.*, 47 (2), 296–307.

[19] Thomas, D.M., Mechery, J., and Paulose, S.V., 2016, Carbon dioxide capture strategies from flue gas using microalgae: A review, *Environ. Sci. Pollut. Res.*, 23 (17), 16926–16940.

[20] Aminu, M.D., Nabavi, S.A., Rochelle, C.A., and Manovic, V., 2017, A review of developments in carbon dioxide storage, *Appl. Energy*, 208, 1389–1419.

[21] Goh, K., Karahan, H.E., Yang, E., and Bae, T.H., 2019, Graphene-based membranes for CO_2/CH_4 separation: Key challenges and perspectives, *Appl. Sci.*, 9 (14), 2784.

[22] Liu, Y., Wang, S., Meng, X., Ye, Y., Song, X., Liang, Z., and Zhao, Y., 2020, Molecular expansion for constructing porous organic polymers with high surface areas and well-defined nanopores, *Angew. Chem., Int. Ed.*, 59 (44), 19487–19493.

[23] He, Y., Zhou, W., Yildirim, T., and Chen, B., 2013, A series of metal–organic frameworks with high methane uptake and an empirical equation for predicting methane storage capacity, *Energy Environ. Sci.*, 6 (9), 2735–2744.

[24] Kong, G.Q., Han, Z.D., He, Y., Ou, S., Zhou, W., Yildirim, T., Krishna, R., Zou, C., Chen, B., and Wu, C.D., 2013, Expanded organic building units for the construction of highly porous metal–organic frameworks, *Chem. - Eur. J.*, 19 (44), 14886–14894.

[25] Peng, Y., Krungleviciute, V., Eryazici, I., Hupp, J.T., Farha, O.K., and Yildirim, T., 2013, Methane storage in metal–organic frameworks: Current records, surprise findings, and challenges, *J. Am. Chem. Soc.*, 135 (32), 11887–11894.

[26] Tran, Y.B.N., Nguyen, P.T., Luong, Q.T., and Nguyen, K.D. 2020, Series of M-MOF-184 (M = Mg, Co, Ni, Zn, Cu, Fe) metal–organic frameworks for catalysis cycloaddition of CO_2, *Inorg. Chem.*, 59 (22), 16747–16759.

[27] Ahmed, D., El-Hiti, G., Yousif, E., Hameed, A., and Abdalla, M., 2017, New eco-friendly phosphorus organic polymers as gas storage media, *Polymers*, 9 (8), 336.

[28] Liu, B., Yao, S., Shi, C., Li, G., Huo, Q., and Liu, Y., 2016, Significant enhancement of gas uptake

capacity and selectivity via the judicious increase of open metal sites and Lewis basic sites within two polyhedron-based metal–organic frameworks, *Chem. Commun.*, 52 (15), 3223–3226.

[29] Wardani, A.R., and Widiastuti, N., 2016, Synthesis of zeolite-X supported on glasswool for CO_2 capture material: Variation of immersion time and NaOH concentration at glasswool activation, *Indones. J. Chem.*, 16 (1), 1–7.

[30] Ediati, R., Mukminin, A., and Widiastuti, N., 2017, Impregnation nickel on mesoporous ZSM-5 templated carbons as a candidate material for hydrogen storage, *Indones. J. Chem.*, 17 (1), 30–36.

[31] Ahmed, D.S., Mohammed, A., Husain, A.A., El-Hiti, G.A., Kadhom, M., Kariuki, B.M., and Yousif, E., 2022, Fabrication of highly photostable polystyrene films embedded with organometallic complexes, *Polymers*, 14 (5), 1024.

[32] Bardestani, R., Patience, G.S., and Kaliaguine, S., 2019, Experimental methods in chemical engineering: Specific surface area and pore size distribution measurements—BET, BJH, and DFT, *Can. J. Chem. Eng.*, 97 (11), 2781–2791.

[33] Thommes, M., Kaneko, K., Neimark, A.V., Olivier, J.P., Rodriguez-Reinoso, F., Rouquerol, J., and Sing, K.S.W., 2015, Physisorption of gases, with special reference to the evaluation of surface area and pore size distribution (IUPAC Technical Report), *Pure Appl. Chem.*, 87 (9-10), 1051–1069.

[34] Sreethawong, T., Suzuki, Y., and Yoshikawa, S., 2005, Synthesis, characterization, and photocatalytic activity for hydrogen evolution of nanocrystalline mesoporous titania prepared by surfactant-assisted templating sol–gel process, *J. Solid State Chem.*, 178 (1), 329–338.

[35] Trickett, C.A., Helal, A., Al-Maythalony, B.A., Yamani, Z.H., Cordova, K.E., and Yaghi, O.M., 2017, The chemistry of metal–organic frameworks for CO_2 capture, regeneration and conversion, *Nat. Rev. Mater.*, 2 (8), 17045.

[36] Ahmed, A.J., Alias, M., Ahmed, D.S., Abdallh, M., Bufaroosha, M., Jawad, A.H., and Yousif, E., 2023, Investigating CO_2 storage properties of Pd(II) and Co(II) chelates of a Schiff's base ligand, *J. Umm Al-Qura Univ. Appl. Sci.*, 9 (1), 96–104.

[37] Kazemi, S., and Safarifard, V., 2018, Carbon dioxide capture on metal-organic frameworks with amide-decorated pores, *Nanochem. Res.*, 3 (1), 62–78.

[38] Saleh, T., Yousif, E., Al-Tikrity, E., Ahmed, D., Bufaroosha, M., Al-Mashhadani, M., and Yaseen, A., 2022, Design, synthesis, structure, and gas (CO_2, CH_4, and H_2) storage properties of porous imine-linkage organic compounds, *Mater. Sci. Energy Technol.*, 5, 344–352.

[39] Yaseen, A.A., Yousif, E., Al-Tikrity, T.B., Kadhom, M., Yusop, M.R., and Ahmed, D.S., 2022, Environmental performance of alternative Schiff bases synthesis routes: A proposal for CO_2 storages, *Pollution*, 8 (1), 239–248.

[40] Mahdi, S.A., Ahmed, A.A., Yousif, E., Ahmed, D., Al-Mashhadani, M.H., and Bufaroosha, M., 2022, Comarine derivatives designed as carbon dioxide and hydrogen storage, *Mater. Sci. Energy Technol.*, 5, 197–207.